Nano/Micro-scale friction properties of Silicon and Silicon coated with Chemical Vapor Deposited (CVD) Self-assembled monolayers

Eui-Sung Yoon[†], R. Arvind Singh, Hyun-Jin Oh, Hung-Gu Han and Hosung Kong

Tribology Research Center, Korea Institute of Science and Technology

Abstract: Nano/micro-scale friction properties were investigated on Si (100) and three self-assembled monolayers (SAMs) (PFOTC, DMDM, DPDM) coated on Si-wafer by chemical vapor deposition technique. Experiments were conducted at ambient temperature ($24 \pm 1°C$) and humidity ($45 \pm 5\%$). Friction at nano-scale was measured using Atomic Force Microscopy (AFM) in the range of 0-40nN normal loads. In both Si-wafer and SAMs, friction increased linearly as a function of applied normal load. Results showed that friction was affected by the inherent adhesion in Si-wafer, and in the case of SAMs the physical/chemical structures had a major influence. Coefficient of friction of these test samples at the micro-scale was also evaluated using a micro-tribotester. It was observed that SAMs had superior frictional property due to their low interfacial energies. In order to study the effect of contact area on coefficient of friction at the micro-scale, friction was measured for Si-wafer and DPDM against Soda Lime balls (Duke Scientific Corporation) of different radii (0.25 mm, 0.5 mm and 1 mm) at different applied normal loads (1500, 3000 and 4800 mN). Results showed that Si-wafer had higher coefficient of friction than DPDM. Further, unlike that in the case of DPDM, friction in Si-wafer was severely influenced by its wear. SEM evidences showed that solid-solid adhesion was the wear mechanism in Si-wafer.

Key words: Nano, micro, friction, tribology, AFM, SEM

Introduction

Self-assembled monolayers, popularly known as 'SAMs' are molecular assemblies that form spontaneously by adsorption to substrates through high affinity chemisorption [1]. Their conventional applications are in the areas of bio/chemical and optical sensors, and for use as drug delivery vehicles [1]. In 1996, Linford and Chidsey [2] demonstrated for the first time that robust monolayers can be prepared and could be bonded to silicon substrates. Since then, these molecular assemblies have found their niche as solid lubricants in MEMs tribology [3]. In MEMs devices, the surface area to volume ratio is large due to the scaling law [3]. Moreover, due to lateral and vertical gaps (clearances) between components being around 1 mm [3], conventional liquid lubricants cannot be used, as they cause liquid-mediated adhesion leading to high static friction [4]. Further, during sliding, frictional effects not only due to external load but also due to the intrinsic liquid-mediated adhesive force needs to be overcome. Under such conditions, SAMs provide an ideal solution for lubrication [3,4] owing to their properties such as thermodynamic stability, formation of close packed structures, hydrophobicity and strong bonding (chemisorption) to the substrates [3,4].

For SAMs to be ideal candidates as lubricants-to mitigate friction and wear, (i) the head group should be a polar group, for it provides strong adherence to the substrate via a chemical bond and (ii) the terminal group (tail group) of the organic molecular chain should be a non-polar group [3]. An in depth overview on various end and head groups, and classes of SAMs can be found in Ulmann's report [1]. Roya Maboudhian et al. [3] and Komvopolous [5] provide insightful reviews on the tribological challenges in MEMs with the main focus on the evaluation of SAMs as lubricants. From their reports it is seen that the tricholorosilane class of SAMs exhibit the best performance, but are difficult to produce due to their sensitivity to water content and humidity during their preparation [1]. SAMs can be produced by various methods such as dipping, microcontact printing, sol gel, spin coating and by chemical vapor deposition [1,3-6].

In the present work, we have investigated the nano/micro-frictional properties of three SAMs namely, Perflouro-octyltricholorosilane ($C_8F_{13}H_4SiCl_3$, PFOTC), DimethylDimethoxysilane ($C_4H_{12}O_2Si$, DMDM) and DiphenylDimethoxysilane ($C_9H_{14}O_3Si$, DPDM) coated on Si-wafer by the chemical vapor deposition (CVD) technique. In this paper, the underlying mechanisms that influence the friction at nano/micro-scales in these SAMs have been reported. Further, the effect of contact area on the micro-friction property of the DPDM, in comparison with that of the un-coated Si-wafer is also presented.

Experimental

SAMs Preparation

Three different SAMs namely, Perflouro-octyltricholorosilane ($C_8F_{13}H_4SiCl_3$, PFOTC), DimethylDimethoxysilane ($C_4H_{12}O_2Si$,

[†]Corresponding author; Tel: 82-2-958-5651, Fax: 82-2-958-5659
E-mail: esyoon@kist.re.kr

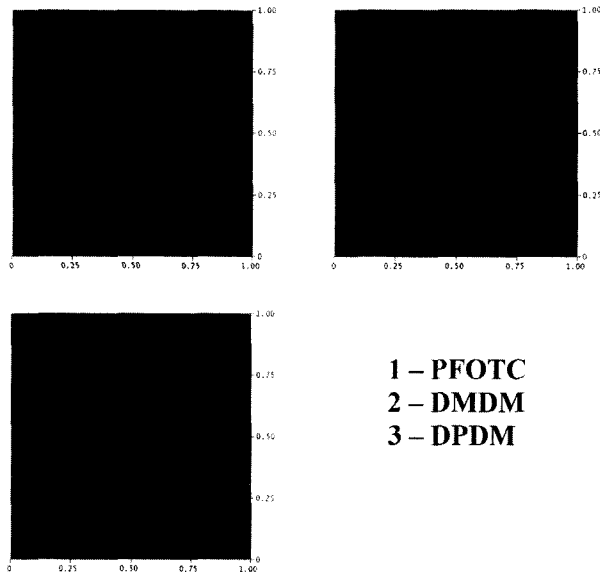**Table 1. Details of preparation conditions of SAMs**

Name	Boiling Point (°C)	Temperature (°C)	Time (Hours)
PFOTC	192	100	2
DMDM	82	50	3
DPDM	176	100	3

Fig. 1. Schematic of structures of SAMs.

Fig. 2. A view of AFM used for the measurement of nano-friction.

Fig. 3. A close-up view of the ball-on-flat type micro-tribotester.

DMDM) and DiphenylDimethoxysilane ($C_9H_{14}O_3Si$, DPDM) were coated on Si-wafer ((100), produced by LG Siltron) by the chemical vapor deposition (CVD) technique. Prior to the coating, the Si-wafers were cleaned in Pirahna solution (H_2SO_4 : H_2O_2 in the ratio 7 : 3) for about 30 minutes at a temperature of about 85°C. Subsequently, they were ultra-sonically cleaned with isopropyl alcohol before being placed in the CVD reactor. The detailed procedure regarding the coating is given elsewhere [7]. Table 1 shows the temperature and time duration at which the SAMs were deposited on Si-wafer in the CVD reactor. The choice of the temperature mainly depends upon the boiling point of the precursor molecules (Table 1). Figure 1 shows the schematic of the structure of the SAMS used in the present study.

Test apparatus

Friction measurements at nano-scale

Nano-scale friction tests were conducted using a commercial Atomic Force Microscope (AFM) (Multimode SPM, Nanoscope IIIa, Digital Instruments). A view of the AFM used in the present study is shown in Fig. 2. The friction force was measured in LFM (Lateral Force Microscope) mode. Friction measurements were made at applied normal loads in the range of 0-40 nN. Measurements were conducted at the scanning speed of 2 mm/s for the scan size of 1 mm × 1 mm using a contact mode type Si_3N_4 tip (NPS 20) that had a nominal spring constant 0.58 N/m. Each test was repeated for 15 times and the average values were plotted.

Friction measurements at micro-scale

Micro-scale friction tests were performed with a ball-on-flat type micro-tribotester (Fig. 3) under reciprocating motion. Two different sets of experiments were conducted: (i) friction was measured for Si-wafer and for the SAMs against a 2 mm diameter Si_3N_4 ball (applied normal load: 4000 mN, sliding speed: 3 mm/sec, scan length: 3 mm) (ii) In order to study of the effect of contact area at the micro-scale, friction was measured for Si-wafer and DPDM against Soda Lime balls (Duke Scientific Corporation) of different radii (0.25 mm, 0.5 mm and 1 mm). Tests were also conducted at three different applied normal loads (1500, 3000 and 4800 mN) for duration of about 30 minutes (sliding speed: 1 mm/sec, scan length: 3 mm). Tests were repeated more than three times and the average values were plotted. All experiments mentioned above, at nano- and micro-scales were conducted at ambient temperature (24 ± 1°C) and humidity (45±5%).

Results and Discussion

Figure 4 shows the topography of the SAMs taken in AFM in

Fig. 4. A close-up view of the ball-on-flat type micro-tribotester.

Table 2. Properties of test specimens

Material	E (GPa)	PR	R (nm)	WCA (Deg)	IE (mN/m)
Si-Wafer	165	0.28	0.15	22	72
Soda Lime	68	0.16	-	-	-
PFOTC	-	-	0.20	106	-
DMDM	-	-	0.17	82	-
DPDM	-	-	0.18	88	-

E: Young's Modulus, PR: Poisson's Ratio, R: Roughness, WCA: Water Contact Angle, IE: Interfacial Energy

a scan area of 1 mm × 1 mm, at the data scale of 100 nm. It is interesting to note that all the SAMs exhibited uniform coating. Further, in the present case, particles (agglomerates) are absent, which in the dipping method is a regular feature that forms because of polymerization during coating. The absence of particle formation is an important difference between the two methods namely the dipping method and the CVD method [6,7]. Table 2 shows the properties of test specimens used.

Friction at nano-scale

Figure 5 shows the variation of friction at nano-scale for Si-wafer and the SAMs. From the figure it is worth noting that the friction force exists even at the zero applied normal load. This is mainly attributed to the influence of the intrinsic adhesive force on the friction force [8]. This adhesive force arises due to the contribution of various attractive forces such as capillary, electrostatic, van der Waal and chemical bonding under different circumstances [3]. In Si-wafer, owing to its hydrophilic nature (Table 2, 3, 9) it is considered that the capillary force due to the formation of meniscus-bridge (condensation of water from the environment) between the tip and the sample, contributes to a major extent. Van der Waal

1 – PFOTC
2 – DMDM
3 – DPDM
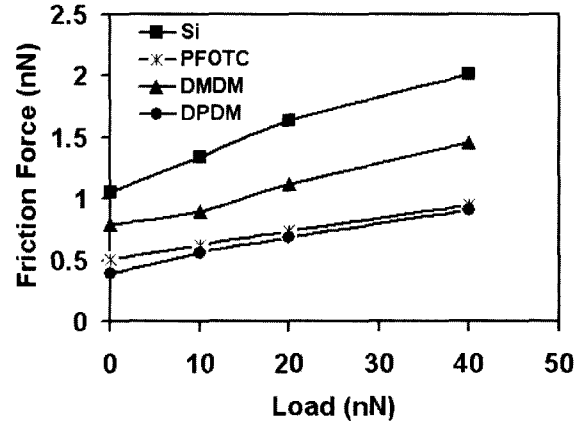
Fig. 5. Friction force as a function of applied normal load measured using AFM.

forces also contribute [10], but their magnitude is less when compared to that of the capillary force [3]. In contrast to Si-wafer, SAMs are hydrophobic in nature (Table 2) and hence, capillary force gets suppressed to a large extent. Friction in nano-scale is in a regime where the contribution from intrinsic adhesion can outweigh those from the asperity deformation and ploughing [3,11]. In the present case, the applied normal load has been limited to 40nN, in an effort not to deform or wear the SAMs, but rather to probe the frictional properties of only the outermost portions of the SAMs. Studies [12] have shown that substantial deformation of monolayers occurs at loads greater than the loads used in the present case. Further, as seen in Fig. 5, the approximately linear response of friction force versus applied load indicates that there has been no significant deformation or wear of these monolayers. In the present case where the deformation is almost absent, the friction force is strongly influenced by the intrinsic adhesion [3,11], thus rendering the SAMs to exhibit lower friction force than the Si-wafer.

Another strong reason for the SAMs to exhibit lower friction force than the Si-wafer is their smaller real area of contact. From Fig. 5 it is observed that for both Si-wafer and the SAMs, the friction force increases linearly with the applied normal load. These trends could be explained by considering the fundamental law of friction given by Bowden and Tabor [13]. According to this law, the friction force is directly dependent on the real area of contact, for the case of a single asperity contact. Equation 1 gives the expression for the friction force.

$$F_f = \tau A_r \qquad (1)$$

Where, τ is the shear strength, an interfacial property and A_r the real area of contact.

The behavior of the friction force in Si-wafer and SAMs is very much consistent with this law of friction, as in both these materials the friction force increases with the increase in the real area of contact. Assuming the contact at nano-scale to be a pseudo-single asperity contact, the real area of contact can be estimated from the JKR equation (2) [14] for Si-wafer, as it exhibits high interfacial energy (lower water contact angle)
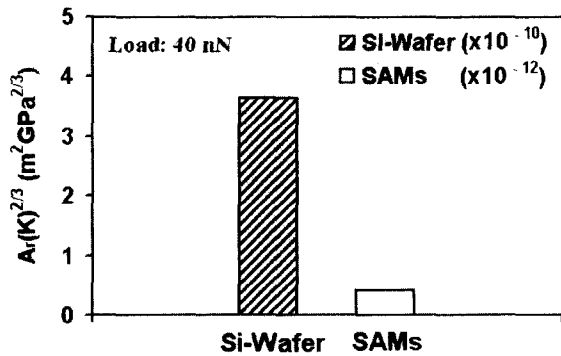
Fig. 6. Estimated $A_r(K)^{2/3}$ for Si-wafer and SAMs at nano-scale (Normal Load: 40 nN).

(Table 2). To estimate the real area of contact in SAMs, the Hertzian equation (only the first term in the eq. 2) is used as they have low interfacial energies (higher water contact angles), which could be more than one order less when compared to that of Si-wafer [15].

$$A_r = \pi [R/K (F_n + 6\pi\gamma R + [12\pi\gamma R F_n + (6\pi\gamma R)^2]^{1/2})]^{2/3} \quad (2)$$

Where, R is the size of the tip, K the effective elastic modulus, F_n the applied normal load and g, the interfacial energy of the material.

For SAMs, the values of Young's modulus and Poisson's ratio are unavailable and hence, we estimate $A_r(K)^{2/3}$ for both the Si-wafer and the SAMs. This would provide a first order comparison between the contact area of Si-wafer and SAMs. Figure 6 shows $A_r(K)^{2/3}$ estimated for these two different kinds of materials, at the applied normal load of 40 nN. It is seen from the figure that Si-wafer exhibits higher contact area than the SAMs, which explains for its higher friction force when compared to that of the SAMs (Fig. 5).

From Fig. 5 it is also seen that both PFOTC and DPDM show lower friction force when compared to DMDM. DPDM shows low friction owing to the nature of its benzene ring (Fig. 1). Rings are expected to be stiff (probably because of their saturated bonds (double bonds)); therefore, their frictional properties are expected to be superior to that of linear molecular structures [16]. Overney *et al.* [17] too have observed similar relation between the friction and stiffness in their work on phase-separated monolayers. Superior friction properties of phenyl terminated SAMs due to the influence of rings has also been observed earlier by Bhushan *et al.* [18]. Further, the low friction values exhibited by PFOTC could be attributed to its structure of long carbon chain (Fig. 1). It is well known that long carbon chain molecular assemblies exhibit lower friction force when compared to assemblies with short carbon chain [4]. Furthermore, what is interesting here is that, although PFOTC has long chain structure than DMDM and DPDM, its friction value is not the least. This could be attributed to the presence of fluorine atom in its chemical structure. Fluorine atoms have larger Van der Waals radii [12,19]. Consequently, they interact more strongly with the neighboring chains, giving rise to long-range multi-molecular interactions [12,19]. To overcome the energetic barrier due to
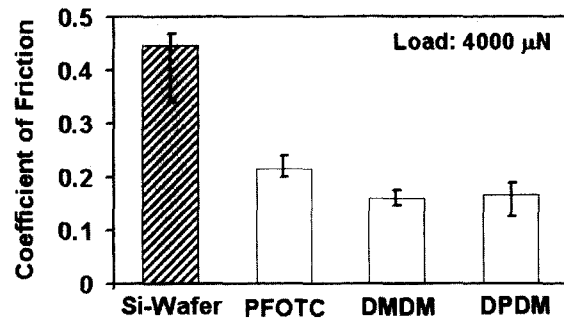

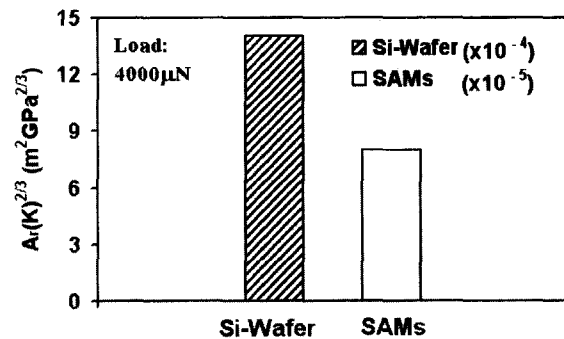Fig. 7. Friction Coefficient measured at micro-scale (Normal load: 4000 mN).

Fig. 8. Estimated $A_r(K)^{2/3}$ for Si-wafer and SAMs at micro-scale (Load: 4000 mN).

the long-range multi-molecular interactions more energy gets imparted to the film during sliding and results in higher frictional property. This explains the reason why the friction in PFOTC is not the least, although it has the long carbon chain structure [12,19].

Friction at micro-scale

Comparison between the coefficient of friction in SAMs

Figure 7 shows the coefficient of friction at micro-scale of Si-wafer and SAMs. From the figure it could be observed that SAMs show lower values of coefficient of friction than that of the Si-wafer. This is mainly attributed to their smaller contact areas (Fig. 8) in comparison to that of the Si-wafer, which in turn is due to their low interfacial energies [15]. Figure 8 shows $A_r(K)^{2/3}$ estimated for Si-wafer and SAMs at micro-scale. These estimations have been done on similar lines as explained in Section 3.1.

From Fig. 7, it is also seen that there is no significant difference between the coefficient of friction values for DMDM and DPDM. As mentioned earlier in Section 3.1, the difference in the frictional behavior between these two SAMs was basically due to the difference in their terminal groups. This difference was markedly recorded at the nano-scale, as the probe (AFM tip), the applied load and the contact between the probe and the sample were all at a finer scale. In the present case, at micro-level, unlike at the nano-scale, all the three above-mentioned parameters namely, the probe size (ball), the applied normal load and the contact area between them are all at a coarser level. Coupled with this, under micro-
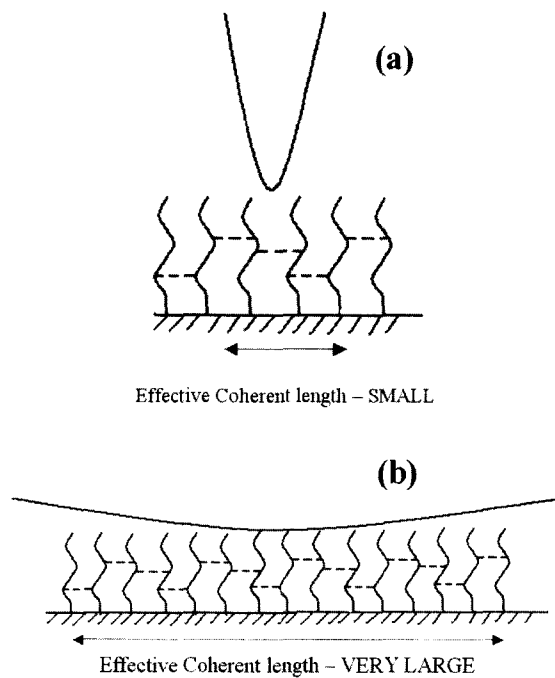
Effective Coherent length – SMALL

(b)

Effective Coherent length – VERY LARGE

Fig. 9. Schematic depiction of effective coherent length in PFOTC at (a) nano-scale and (b) micro-scale.

Fig. 10. Coefficient of friction measured at micro-scale in Si-wafer.

Fig. 11. Coefficient of friction measured at micro-scale in DPDM.

loads, the bi-directional sliding for long duration (30 minutes) would induce deformations unseen at the nano-scale. All these factors together make the influence of the finer aspects of SAMs structures (DMDM, DPDM) on their frictional properties undetectable at micro-scale. In comparison to that of DMDM and DPDM, PFOTC shows high- values of coefficient of friction; even though it has long carbon chain (Fig. 7) and that the long chain structures usually reduce the values even at micro-scale [4]. The reason that could possibly explain for the high frictional value of PFOTC is the presence of the fluorine atom in its chemical structure. As mentioned earlier in Section 3.1, fluorine terminated SAMs exhibit higher frictional properties than the hydrogen terminated ones due to the larger Van der Waals radii of the fluorine atom [12,19]. The larger Van der Waals radii of fluorine atoms effect long-range multi-molecular interactions in the plane of CF_3 groups. These long-range interactions correspond to longer coherence lengths that act as energetic barriers [12]. In order to overcome these energetic barriers more energy gets imparted during sliding, resulting at higher friction. Such an effect gets pronounced at the micro-scale, as longer coherent lengths exist over larger contact area (Fig. 9), resulting at higher frictional property.

Effect of contact area on the coefficient of friction

Figures 10 and 11 show the variation of the coefficient of friction at micro-scale as a function of applied normal load, for various ball sizes in the case of Si-wafer and DPDM respectively. It is seen from the figures that the coefficient of friction increases with the ball size in both the specimens. Further, DPDM shows lower values in comparison with that of Si-wafer, under all the test conditions. Another important observation was that the Si-wafer exhibited significant wear,
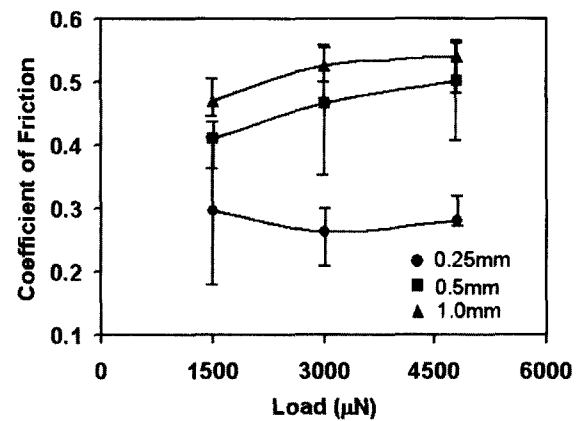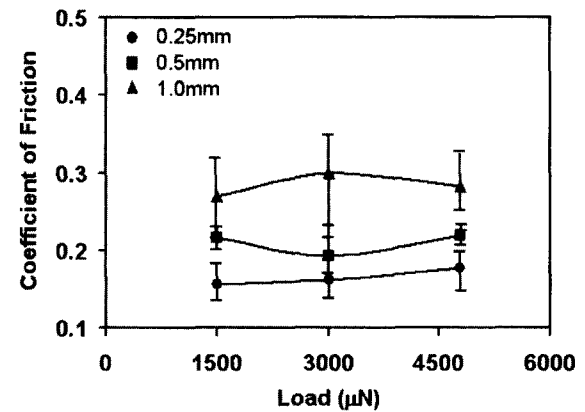
which was clearly visible even to the naked eye. Such a severe wear that could even be recognized by the naked eye was absent in DPDM. Although, deformations at this scale cannot be ruled out in DPDM, wear in the case of Si-wafer was comparatively severe. Figures 12a shows the wear track seen on Si-wafer tested against glass balls of radius 1 mm at 3000 mN. Wear debris are seen on these tracks. Figure 12b is a micrograph that shows debris smeared at the center of the wear track. These evidences indicate that wear occurred in Si-wafer by solid-solid adhesion. This could be attributed to it high interfacial energy, which supports such a mechanism. Furthermore, it could be stated that friction in Si-wafer was influenced by its wear. In the past, experiments conducted by Gardos [20] have shown that Si-wafer exhibits high adhesive friction followed by shear-induced micro cracking in the wake of the sliding. Figure 13 shows $A_r(K)^{2/3}$ estimated for Si-wafer and DPDM (estimated on similar lines as explained previously) for different ball sizes at 3000 mN loads. The estimation of $A_r(K)^{2/3}$ for Si-wafer was done using the JKR model as it includes the contribution of adhesion, whereas for DPDM, the Hertzian model was used. It is seen from this figure that Si-wafer exhibits higher contact area than DPDM at all ball sizes owing to its high interfacial energy. Further, the increase in the contact area with the increase in the ball size
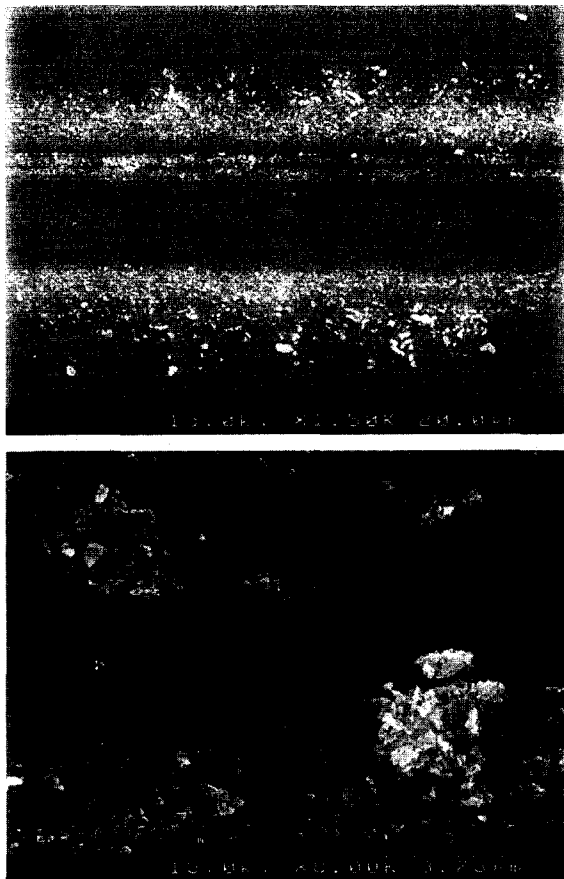
Fig. 12. (a) SEM micrographs of wear track on Si-wafer (1 mm ball radius, 3000 mN) (b) Wear debris at the center of the wear track.

Fig. 13. Estimated $A_r(K)^{2/3}$ for Si-wafer and DPDM at micro-scale (Load: 3000 mN).

directly assists the adhesive mechanism in Si-wafer and increases the friction force, thereby increasing its coefficient of friction. In the case of DPDM although the increase in the contact area with the increase in ball size increases the coefficient of friction, its lower interfacial energy [15] affects lower contact area in comparison to that of Si-wafer leading to lower values of coefficient of friction than that of the Si-wafer.

Conclusions

Frictional properties at nano/micro-scale of three SAMs coated on Si-wafer by the chemical vapor deposition (CVD) method were evaluated. The following are the conclusions drawn from the present investigation:

(1) At nano-scale, SAMs exhibit superior frictional property than Si-wafer owing to their smaller contact area effected by their lower interfacial energies.

(2) In SAMs, friction at nano-scale is influenced by the structure of their assembly and their end terminal group. Long carbon chain morphology (PFOTC) and phenyl-terminated monolayers (DPDM) exhibit lower friction.

(3) Similar to that at nano-scale, SAMs exhibit superior frictional property than Si-wafer even at the micro-scale owing to their smaller contact area effected by their lower interfacial
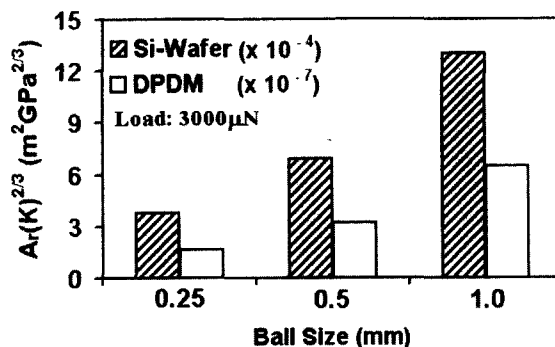
energies.

(4) Unlike at the nano-scale, the finer influence of the end terminal group on the frictional property in DMDM and DPDM is not detectable at the micro-scale. PFOTC exhibits higher frictional value because of its larger Van der Waal radius.

References

1. Ulman, Abraham., "Formation and Structure of Self-Assembled Monolayers", Chem. Rev. 96, pp.1533-1554, 1996.
2. Linford, M.R, Chidsey., C.E.D., J. Am. Chem. Soc. 115, p. 12631, 1993.
3. Maboudian, Roya, Roger, Howe, T., "Critical Review: Adhesion in surface micromechanical structures", J. Vac. Sci. Technol. B 15 (1), pp. 1-20, 1997.
4. Bhushan, Bharat., "Modern Tribology Handbook", Volume 2, CRC Press, Boca Raton, Florida, 2001.
5. Komvopoulos, K., "Surface engineering and microtribology for microelectromechanical systems", Wear 200, pp. 305-327, 1996.
6. Ashurst, Robert, W, Carraro, C, Maboudian, R, Frey, W., "Wafer level anti-stiction coatings for MEMS", Sensors and Actuators A 104, pp. 213-221, 2003.
7. Oh, Hyun-Jin, Yoon, Eui-Sung, Han, Hung-Gu, Kong, Hosung., "Micro/nano adhesion and friction properties of SAMs with different head and functional group according to the coating methods", KSTLE-38th Spring Conference, June 11, Seoul, pp. 177-184, 2004.
8. Bharat Bhushan, Ashok V. Kulkarni., "Effect of normal load on microscale friction measurements", Thin Solid Films 278, pp 49-56, 1996.
9. Bhushan, B, Sundararajan, S., "Micro/Nanoscale Friction and Wear mechanisms of thin films using atomic force and friction force microscopy," Acta mater. 46 (11), pp.3793-3804, 1998.
10. Bhushan, Bharat, Dandavate, Chetan., "Thin-film friction and adhesion studies using atomic force microscopy", Journal of Applied Physics 87 (3), pp. 1201-1210, 2000.
11. Mastrangelo, C.H., Tribol. Lett. 3, pp. 223-238, 1997.
12. Kim, Hyun, I, Koini, Thomas, Lee, Randall, T, Perry, Scott, S., "Systematic Studies of the Frictional Properties of Fluorinated Monolayers with Atomic Force Microscopy: Comparison of CF₃- and CH₃-Terminated Films", Langmuir 13, pp. 7192-7196, 1997.
13. Bowden, F. P, Tabor, D., "The friction and lubrication of solids", Clarendon Press, Oxford, 1950.
14. Johnson, K. L, Kendall, K, Roberts, A.D., "Surface energy and

contact of elastic solid", Proceedings of the Royal Society of London A 324, pp. 301-313, 1971.

15. Maboudian, Roya, Ashrust, Robert, W, Carraro, Carlo, "Tribological challenges in micromechanical systems", Tribol. Lett. 12 (2), pp. 95-100, 2002.

16. Geyer, Stadler, W, Eck, V, Zharnikov, M, Golzhauser, A, Grunze, M., "Electron-induced crosslinking of aromatic self-assembled monolayers: negative resists for nanolithography", Appl. Phys. Lett. 75, pp. 2401-2403, 1999.

17. Overney, R.M, Meyer, E, Frommer, J, Guntherodt, H.J, Fujihira, M, Takano, H, Gotoh, Y., "Friction measurements on phase-seperated thin films with a modified atomic force microscope", Langmuir 10, p. 1281, 1994.

18. Bhushan, Bharat, Liu, Huiwen., "Nanotribological properties and mechanisms of alkylthiol and biphenyl thiol self-assembled monolayers studied by AFM", Physical Review B 63, p. 245412, 2001.

19. Kim, Hyun, I, Graupe, Michael, Oloba, Olugbenga, Koini, Thomas, Imaduddin, Syed, Lee, Randall, T, Perry, Scott, S., "Molecularly Specific Studies of the Frictional Properties of Monolayer Films: A Systematic Comparison of CF_3-, $(CH_3)_2CH$- and CH_3-Terminated Films", Langmuir 15, pp. 3179-3185, 1999.

20. Gardos, M.N., "Surface chemistry-controlled tribological behaviour of Si and Diamond", Tribology Letters 2, p. 173, 1996.